The Journal of Experimental Biology 210, 4286-4297
Published by The Company of Biologists 2007
doi:10.1242/jeb.009969

Endothelin and endothelin converting enzyme-1 in the fish gill: evolutionary and physiological perspectives

Kelly A. Hyndman* and David H. Evans

Department of Zoology, University of Florida, 221 Bartram Hall, Gainesville, FL 32608, USA and Mount Desert Island Biological Laboratory, Salisbury Cove, ME 04672, USA

*Author for correspondence (e-mail: khyndman@zoo.ufl.edu)

Accepted 24 September 2007

Summary

In euryhaline fishes like the killifish (*Fundulus heteroclitus*) that experience daily fluctuations in environmental salinity, endothelin 1 (EDN1) may be an important regulator molecule necessary to maintain ion homeostasis. The purpose of this study was to determine if EDN1 and the endothelin converting enzyme (ECE1; the enzyme necessary for cleaving the precursor proendothelin-1 to EDN1) are present in the killifish, to determine if environmental salinity regulates their expression, and to examine the phylogenetic relationships among the EDNs and among the ECEs. We sequenced killifish gill cDNA for two *EDN1* orthologues, *EDN1A* and *EDN1B*, and also sequenced a portion of *ECE1* cDNA. *EDN1A* and *ECE1* mRNA are expressed ubiquitously in the killifish while *EDN1B* mRNA has little expression in the killifish opercular epithelium or gill. Using *in situ* hybridization and immunohistochemistry, EDN1 was localized to large round cells adjacent to the mitochondrion-rich cells of the killifish gill, and to lamellar pillar cells. In the gill, *EDN1A* and *EDN1B* mRNA levels did not differ with acute (<24 h) or chronic (30 days) acclimation to seawater (SW); however, *EDN1B* levels increased threefold post SW to freshwater (FW) transfer, and *ECE1* mRNA levels significantly increased twofold over this period. *ECE1* mRNA levels also increased sixfold over 24 h post FW to SW transfer. Chronic exposure to SW or FW had little effect on *ECE1* mRNA levels. Based upon our cellular localization studies, we modeled EDN1 expression in the fish gill and conclude that it is positioned to act as a paracrine regulator of gill functions in euryhaline fishes. It also may function as an autocrine on pillar cells, where it is hypothesized to regulate local blood flow in the lamellae. From our phylogenetic analyses, ECE is predicted to have an ancient origin and may be a generalist endoprotease in non-vertebrate organisms, while EDNs are vertebrate-specific peptides and may be key characters in vertebrate evolution.

Key words: endothelin, endothelin converting enzyme, *Fundulus heteroclitus*, killifish, gill.

Introduction

Endothelin (EDN) is a family of three autocrine/paracrine peptides (EDN1, EDN2 and EDN3) that function in a variety of physiological processes such as the regulation of vascular tone (Yanagisawa et al., 1988) and natruresis in the kidney (Zeidel et al., 1989). Endothelins are translated as ~200 amino acid (aa) preproendothelins (preproEDN) that are initially cleaved by a furin-like enzyme (Yanagisawa et al., 1988) to form the relatively inactive 38 aa proendothelin (proEDN, also known as Big-EDN) (Kimura et al., 1989). Proendothelin is further cleaved to form the active 21 aa EDN by the endothelin converting enzyme (ECE-1 and/or ECE-2) (Shimada et al., 1994; Xu et al., 1994). In mammals, actions of EDNs are mediated *via* two G-protein coupled receptors: endothelin A receptor (EDNRA), which preferentially binds EDN1 (Arai et al., 1990), and endothelin B1 receptor (EDNRB1), which binds all three EDNs with equal affinity (Sakurai et al., 1990). In non-mammalian vertebrates, EDNs also equally bind to a third G-protein coupled receptor, endothelin B2 receptor (EDNRB2) (Lecoin et al., 1998), and in amphibians EDN3 binds to an amphibian-specific receptor termed endothelin C receptor (EDNRC) (Karne et al., 1993).

Preproendothelin genes have been found in all major gnthastome clades (Fig. 1), and there is evidence for EDN1 regulation of vascular tone in fishes (Olson et al., 1991; Evans et al., 1996; Evans, 2001; Evans and Harrie, 2001; Wang et al., 2001). In addition, EDN1 inhibition of transport by the multidrug resistance-association protein was demonstrated in shark (*Squalus acanthias*) rectal tubules (Miller et al., 2002) and killifish (*Fundulus heteroclitus*) renal tubules (Masereeuw et al., 2000). Recently, Evans et al. (Evans et al., 2004) determined that exogenous (mammalian) EDN1 inhibited net chloride transport in the killifish opercular epithelium, a tissue used as a model for the SW teleost gill (Karnaky et al., 1977). In teleosts, the gill is the main site for ion balance, nitrogen excretion, acid–base regulation and gas exchange (Evans et al., 2005). Estuarine euryhaline fishes like the killifish (*Fundulus heteroclitus*) encounter varying environmental salinities

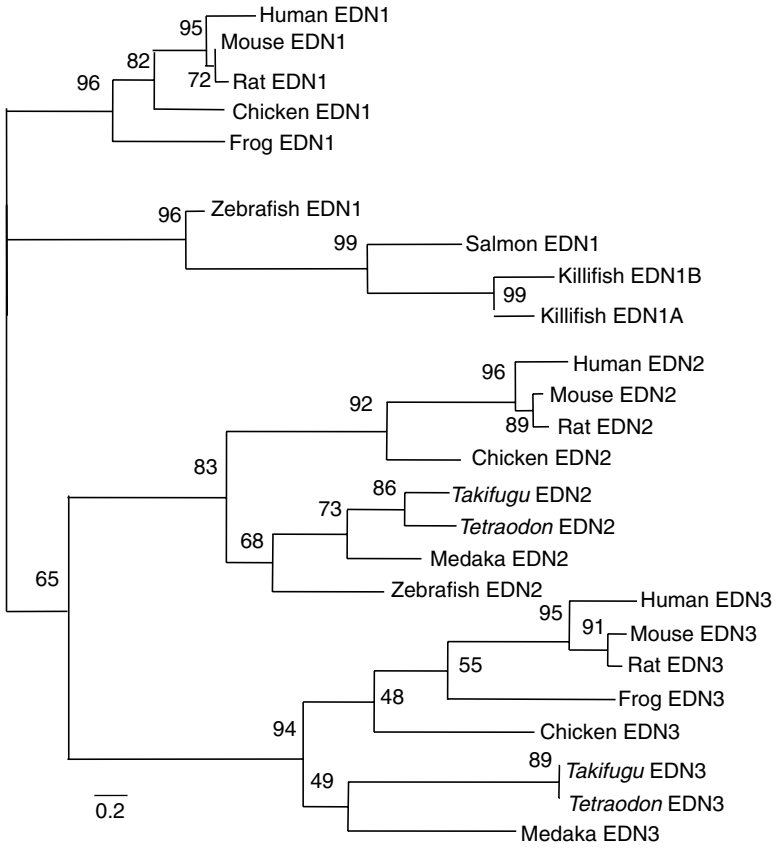

Fig. 1. Maximum likelihood analyses of the vertebrate preproendothelin amino acid sequences. Following the WAG model of amino acid substitutions (Whelan and Goldman, 2001) and a gamma=1.023, there are three distinct groups of preproendothelins, preproendothelin-1 (abbreviated as only EDN1 to save space), preproendothelin-2 (EDN2) and preproendothelin-3 (EDN3). Numbers at nodes represent the percent bootstrap (BS=500 replications). GenBank accession or Ensembl numbers: Chicken EDN1, XP_418943; chicken EDN2, XP_417707; chicken EDN3, XP_001231488; frog EDN1, AAS13535.1; frog EDN3, AAS13536.1; human EDN1, NP_001946; human EDN2, NP_001947; human EDN3, NP_000105; killifish EDN1A, EU009474; killifish EDN1B, EU009475; medaka EDN1, ENSORLP00000011633; medaka EDN2, ENSORLP00000010557; medaka EDN3, ENSORLP00000011814; mouse EDN1, NP_034234; mouse EDN2, P22389; mouse EDN3, NP_031929; rat EDN1, NP_036680; rat EDN2, NP_036681; rat EDN3, NP_001071118; salmon EDN1, BAF30875.1; *Takifugu* EDN2, NEWSINFRUP00000182956; *Takifugu* EDN3, NEWSINFRUP00000181774; *Tetraodon* EDN3, GSTENT00028275001; *Tetraodon* EDN2, GSTENT00026224001; Zebrafish EDN1, NP_571594; Zebrafish EDN2, NP_001038650. Scale bar represents the number of replacements per site.

throughout the day (Marshall, 2003), resulting in a net gain or loss of ions depending on the water salinity; thus the regulation of gill ion transport is an important mechanism to maintain ionic homeostasis. Evans et al. hypothesized that EDN1 signaling cascades in the gill may be a local regulator of ion balance in fishes (Evans et al., 2004). Thus, the purpose of this study was to determine if EDN1 and ECE1 are produced in the killifish, and secondarily to determine if environmental salinity regulates gill *EDN1* and/or *ECE* mRNA expression. We were also interested in determining the phylogenetic/evolutionary relationships of the EDNs and ECE family of proteins.

Materials and methods

Fish maintenance

Killifish *Fundulus heteroclitus* L. were trapped in North East Creek, Mount Desert Island, ME, USA and maintained in free flowing, 32 p.p.t. seawater (SW) tanks at the Mount Desert Island Biological Laboratory, under a natural summer photoperiod, before being shipped to the University of Florida. There they were maintained in 32 p.p.t., 23°C SW, under a 12 h:12 h light:dark photoperiod. Tank pH was maintained between 7.8 and 8.0, and ammonia, nitrate and nitrite levels were below 1 p.p.m. The fish were fed commercial fish pellets to satiation every other day.

EDN1 cDNA

All protocols and procedures were approved by the Institutional Animal Care and Use Committee at the University of Florida. Previously published molecular protocols were used (Hyndman et al., 2006). Killifish were decapitated, and the gills of the right side were removed and snap frozen in liquid nitrogen. Total RNA was then isolated with TRI-reagent (Sigma, St Louis, MO, USA), and 5′ and 3′ RACE cDNA was synthesized from 4 μg of total RNA using a GeneRacer™ Kit (Invitrogen, Carlsbad, CA, USA) according to the manufacturer's protocols. Published degenerate reverse *EDN1* primers (Wang et al., 2006) were used in our initial 5′ Touchdown RACE PCR following Invitrogen's protocols. The polymerase used was 0.625 Units of Ex Taq, hot start, DNA polymerase (Takara Bio, Madison, WI, USA) and the reactions were run in an Express thermocycler (ThermoHybaid, Franklin, MA, USA). The PCR parameters were: 94°C for 2 min, 5 cycles of 94°C for 30 s, 72°C for 30 s, 5 cycles of 94°C for 30 s, 70°C for 30 s, 30 cycles of 94°C for 30 s, 45°C for 30 s, 72°C 30 s, and a final 72°C for 5 min. PCR products were visualized by ethidium bromide staining in 1.5% agarose gels, ligated into pCR®4-TOPO vectors, and transformed into TOP10 chemically competent cells using a TOPO TA Cloning® Kit for sequencing (Invitrogen). Plasmid DNA was then sequenced in both directions at the Marine DNA Sequencing Facility at the Mount Desert Island Biological Laboratory (Salisbury Cove, ME, USA). Once we had the 5′ end, specific killifish *EDN1* primers were designed (Table 1) and 3′ Touchdown RACE PCR was performed to complete the cDNA sequences. The PCR parameters were: 94°C for 2 min, 5 cycles of 94°C 30 s, 72°C for 30 s, 5 cycles of 94°C for 30 s, 70°C for 1 min, 30 cycles of 94°C for 30 s, 50°C for 30 s, 72°C for 1 min, and a final 72°C for 10 min. PCR products were cloned and sequenced as above.

ECE cDNA

To obtain *ECE* cDNA, 4 μg of total gill RNA (extracted as described above) was reverse transcribed using the First-strand cDNA Superscript™ III reverse transcriptase kit (Invitrogen)

Table 1. *Primers used for cloning, tissue distributions and quantitative real-time PCR*

Name	Orientation	Primer (5′→3′ orientation)
3′ EDN1F1†	Sense	GAC GCT CTC CTG GAT CCT CTG CAC AGC T
3′ EDN1F2†	Sense	CAA CAA GCG CTG CTC CTG CGC AAC TTT C
ECEF1*	Sense	CCG GAC TGT CGA CCC ATG YSA NGA YTT
ECEF2*	Sense	CCT GCA TGA ATG AGA CCA AGA THG ARG ARY T
ECER1*	Antisense	CGC ACT TGT GTG GCG GRT TCA TNG G
td EDN1A F1	Sense	CAG TAA CAG AAC CTC TGG CGG A
td EDN1A R1	Antisense	TCC ACG CAG CTG CTA TCA TT
td EDN1B F1	Sense	GTC GGT GTC TGC GTG AAA ATG A
td EDN1B R1	Antisense	CAG ACC GGA GGA TGA AGT TCA G
td ECE F1	Sense	TCC CCT TTC TTC ACT GTG TTT G
td ECE R1	Antisense	CTT CTG GAG GTA CTC TTT GGC A
q EDN1A F1	Sense	TCC AGA GAG CGA AGA GCA TTC C
q EDN1A R1	Antisense	TGA CTC TAT CCG TTT TTG GTG C
q EDN1B F1	Sense	TGA ACT TCA TCC TCC GGT CTG
q EDN1B R1	Antisense	TTT GTC TTC AGC TGC CAC ATG
q ECE1 F1	Sense	CCT GTG ACA CTC AGC GAA TCA
q ECE1 R1	Antisense	CTT CTG GAG GTA CTC TTT GGC A
q L8 F1	Sense	CGT TTC AAG AAA AGG ACG GAG C
q L8 R1	Antisense	GGC GCT GCA GGT GGC GTA G

*Degenerate primers.
†Primers used in RACE-PCR.
td, tissue distributions; q, quantitative real-time PCR.

with oligo-dT primers. Initial degenerate primers used to generate ECE were designed using CODEHOP (Rose et al., 2003) and are recorded in Table 1. PCRs were run on 0.5 μl of the oligo-dT cDNA, with 0.625 units of Ex Taq, hot start (Takara) and standard cycling parameters. PCR products were cloned and sequenced as described above.

Sequence and phylogenetic analysis

Sequence results for each transcript were assembled with GeneTools software (BioTools Inc., Edmonton, Alberta, Canada) and killifish *EDN1* and *ECE1* nucleotide sequences were searched for open reading frames (ORFs). The resulting amino acid translations were analyzed with the basic local alignment search tool (Blast) on the National Center for Biotechnology Information (NCBI) website. The predicted amino acid sequences were aligned with other full-length vertebrate EDN or ECE proteins using Clustal X (Chenna et al., 2003). All sequences were taken from GenBank or the Genome projects in Ensembl (e:!44 April 2007). Preproendothelin-1 sequences from each major vertebrate clade (mammals to teleosts) were separately aligned, and similarities among the sequences highlighted with GeneDoc (available at http://www.psc.edu/biomed/genedoc), including the expected cleavage sites for furin and ECE (Yanagisawa et al., 1988; Opgenorth et al., 1992). To determine the relationship among our sequences and those from other organisms, EDN and ECE alignments were exported to PHYML (Guindon et al., 2005) and a Fast Maximum-Likelihood test was performed, following the WAG model of amino acid substitutions (Whelan and Goldman, 2001) and a calculated gamma of 1.023 and 1.03, respectively. Branches were then tested for statistical significance by bootstrapping with 500 replicates.

Multiple tissue semi-quantitative PCR

To determine the distribution of *EDN1A*, *EDN1B* and *ECE1* mRNA among tissues, relative duplexing semi-quantitative PCR was performed on total RNA from gill, opercular membrane, brain, heart, stomach, intestine and kidney tissue, as described previously (Choe et al., 2004; Choe et al., 2005). Briefly, cDNA was produced from the tissues of a SW killifish as described above, but random hexamer primers (not oligo-dT primers) were used so that ribosomal and messenger RNA would be reverse transcribed. Non-degenerate primer pairs were designed to amplify a product with high efficiency (e.g. high melting temperature), and to minimize the chance of amplifying contaminating genomic DNA, the primer pair was designed to include at least one intron–exon boundary when possible (Table 1). A QuantumRNA™ 18S internal standard primer kit (Ambion, Woodward Austin, TX, USA) was used to control for variability in cDNA quality and quantity between the different tissues tested. Duplexing PCR with primers for 18S and either *EDN1A*, *EDN1B* or *ECE1* were then optimized to ensure that the reactions were terminated during the exponential phase. Lastly, the products were visualized by ethidium bromide staining in 1.5% agarose gels and digitized using the Biorad Gel Doc™ XR System.

Salinity challenges

Killifish were acclimated to SW (approximate concentrations in mmol l^{-1}: Na^+ 517, Ca^{2+} 9, K^+ 12, Cl^- 486) (Choe and Evans,

2003) or freshwater (FW; Gainesville dechlorinated tapwater, approximate concentrations in mmol l^{-1}: Na^+ 4, Ca^{2+} 1, K^+ 0.03, Cl^- 0.40) (Choe and Evans, 2003) for 2 weeks, at which point the SW killifish were transferred into FW (SW→FW) and the FW killifish were transferred into SW (FW→SW). An additional set of killifish were removed and replaced into SW or FW as sham controls (SW→SW and FW→FW, respectively). Immediately after transfer, 5 or 6 killifish from each treatment were sacrificed, the gills excised and snap frozen for RNA extraction and cDNA synthesis. Killifish (*N*=5 or 6/treatment) were further sacrificed at 3, 8 and 24 h post transfer (acute acclimations), as well as 30 days post transfer (chronic acclimation). RNA was extracted from all of the samples and oligo-dT cDNA synthesized as described above.

Quantitative real-time PCR

To determine the effects of environmental salinity on killifish gill *EDN1A*, *EDN1B* and *ECE1* mRNA levels, quantitative real-time PCR (qRT-PCR) was performed. Nondegenerate primers were designed to amplify a product between 50–100 bp across a predicted intron–exon boundary (Table 1). L8 was used as an internal control gene, as previously described (Choe et al., 2005; Choe et al., 2006). Each sample was run in triplicate using 2 μl of 1/10 diluted original cDNA, 7.4 pmol of primers and SYBR® Green Master Mix (Applied Biosystems, Foster City, CA, USA) in a total volume of 25 μl. The cycling parameters used were: an initial denaturing step of 95°C for 10 min, 40 cycles of 95°C for 35 s, 60°C for 30 s and 72°C for 30 s, followed by a melting curve analysis to ensure only one product was amplified. Random samples were also sequenced following qRT-PCR, confirming amplification of the target of interest. To determine the degree of possible genomic contamination, qRT-PCR was run using RNA samples that were not reverse transcribed, and we determined that there was no genomic contamination. All qRT-PCRs were run on a MyiQ quantitative thermocycler (Biorad, Hercules, CA, USA).

Each primer pairs' efficiency was determined by performing a tenfold dilution curve using plasmid cDNA. Efficiency (E) for each primer pair was calculated using the equation: $E=-1+10^{(-1/\text{slope})}$, where 'slope' was the slope of the dilution curve. Each cycle threshold (CT) value was subtracted from a randomly chosen control sample resulting in a ΔCT, and were analyzed using the Pfaffl equation (Pfaffl, 2001): ratio= $E^{\Delta CTtarget}/E^{\Delta CTL8}$. Each Pfaffl ratio was then standardized to the average chronic seawater Pfaffl ratio.

Statistics

Values are expressed as means ± s.e.m. (standard error). For qRT-PCR data, a two-factor ANOVA was performed to determine whether effect of environmental salinity over time differed between SW→FW transfers and SW→SW shams or FW→SW transfers and FW→FW shams. If statistical significance was found a one-factor ANOVA was run to determine the effect of time over a treatment group. Finally, all time points were compared to sham time points with unpaired *t*-tests to determine if salinity transfers altered mRNA expression. All values that did not meet homogeneity or equal variance tests were log transformed to meet the assumptions of the ANOVA; $P=0.05$.

Tissue preparation for in situ hybridization and immunohistochemistry

Killifish gills were fixed in 4% paraformaldehyde in 10 mmol l^{-1} phosphate buffered saline (PBS) pH 7.3, for 24 h, dehydrated in an increasing concentration of ethanol, cleared in Citrisolv (Fisher Scientific, Pittsburgh, PA, USA), and embedded in paraffin wax. The tissue blocks were cut at 7 μm, placed on Superfrost Plus slides (Fisher Scientific), and heated at 37°C overnight.

In situ hybridization

mRNA for *EDN1A*, *EDN1B* and *NKA* (Na^+,K^+-ATPase) mRNA were visualized using *in situ* hybridization. An *ECE1* mRNA probe was not made because our partial sequence of that transcript was from the middle of the sequence, a region that in other fishes is >65% identical to *ECE2*, and we were afraid of the potential cross-reactivity of this probe. Specific digoxigenin (DIG)-RNA probes (sense and antisense) were made against the 3′ end of the transcripts [including untranslated regions (UTRs) for the *EDN*s; these regions were <60% identical]. For *EDN1A* the probe was made from position 520 to the end of the transcript, including the polyA tail (420 bp long). The *EDN1B* probe was made from position 515 up to and including the polyA tail (419 bp). Both of these transcripts were cloned as described above. A killifish *NKA* mRNA probe was also made based upon the complete killifish NKA sequence (AY057072). The probe was made from base pairs 915–3115. This transcript was also cloned and sequenced to ensure it was indeed *NKA*. All of the transcripts were linearized by T3/T7 PCR amplification from the plasmids containing the sequences of interest. DIG-RNA probes were generated by incubating 100–200 ng of the linearized transcripts with the DIG RNA Labeling mix (Roche Applied Science, Indianapolis, IN, USA) following the manufacturer's protocols, at 37°C for 16 h followed by treatment with DNAse for 1 h at 37°C. The DIG-RNA probes were purified using mini Quick Spin RNA columns (Roche) following the manufacturer's instructions, eluted in 80 μl of diethyl pyrocarbonate (DEPC) treated water and stored at –80°C until use.

To determine which gill cells expressed *EDN1A* or *EDN1B* mRNA, gill tissue slides were rehydrated in two changes of Citrisolv, followed by incubation in a series of decreasing concentration of ethanol washes. The slides were placed in sterile 10 mmol l^{-1} PBS and post-fixed in 4% PFA for 10 min at room temperature (25°C). Following this, the slides were rinsed in sterile 10 mmol l^{-1} PBS and incubated in proteinase K (5 mg ml^{-1}) at room temperature for 5 min. Again, they were washed in 10 mmol l^{-1} PBS and post fixed in 4% PFA for 10 min to inactivate the proteinase K. After a final PBS wash, the slides were incubated in prehybridization solution (50% formamide, 10% dextran sulphate, 2% blocking reagent, 0.1% CHAPS, 1% Tween 20, 5 mmol l^{-1} EDTA, pH 8.0, 5× SSC, 50 μg ml^{-1} heparin, 1 mg ml^{-1} tRNA, in DEPC-water) for 2 h at room temperature. Next 200–500 ng of DIG-RNA probes were added to fresh prehybridization solution and the slides were left to incubate at 60°C for 18–24 h. Following this, the tissues were washed for 30 min in 2× SSC at room temperature, 2× SSC at 60°C, two 0.2× SSC 60°C washes, one 0.2× SSC at room temperature and KTB (50 mmol l^{-1} Tris pH 7.5,

100 mmol l^{-1} NaCl and 10 mmol l^{-1} KCl) at room temperature. The tissues were then blocked in 20% normal goat serum diluted in KTB for 1 h at room temperature and incubated in 7.5 U ml^{-1} of sheep anti-DIG-AP, Fab fragments (Roche) diluted in normal goat serum (NGS), overnight at 4°C. The slides were then washed in three changes of KTB and incubated in alkaline phosphatase buffer (100 mmol l^{-1} Tris, pH 9.5, 100 mmol l^{-1} NaCl, 50 mmol l^{-1} $MgCl_2$) for 30 min at room temperature. Visualization of the probes was achieved by incubating the tissues in BCIP/NBT Substrate Kit, 5-bromo-4-chloro-3-indolyl phosphate/nitroblue tetrazolium (Vector Labs, Burlingame, CA, USA) with levamisole, following manufacturer's instructions, at room temperature until the signal developed (2–6 h). Images were captured using an Olympus BX60 light microscope with a Hitachi KP-D50 digital camera. Image contrast and brightness were adjusted with Photoshop CS (Adobe, San Jose, CA, USA).

Immunohistochemistry

Slides were analyzed following published methods (Piermarini et al., 2002; Hyndman et al., 2006). Slides with chronic SW and FW acclimated killifish gill tissue were incubated in primary antibodies: polyclonal, anti-human-proEDN1 (1/1000 dilution) (Phoenix Pharmaceutical, Burlingame, CA, USA) made against the complete 38 aa of human proEDN1, which is 74% identical to both killifish EDN1s. Monoclonal, anti-NKA (α5, 1/1000) was developed by Dr Douglas Fambrough, and was obtained from the Developmental Studies Hybridoma Bank, which was developed under the auspices of the National Institute of Child Health and Human Development of the University of Iowa, Department of Biological Sciences, Iowa City, IA 52242, USA.

Results

Sequence analyses

From the killifish gill we have sequenced two *EDN1* transcripts and designated them *EDN1A* (accession no. EU009474) and *EDN1B* (accession no. EU009475). *EDN1A* is 917 bp with an ambiguous base at position 762 (C or T), and a predicted ORF of 483 bp that translates into a preproendothelin-1A (preproEDN1A) of 189 aa. *EDN1B* is 912 bp with a predicted ORF of 429 bp that translates into a preproendothelin-1B (preproEDN1B) of 143 aa. The predicted cleavage sites in the preproEDN1s for furin and ECE are depicted in Fig. 2A. As found in other vertebrate preproEDN1 peptides, preproEDN1A and preproEDN1B contain the dibasic cleavage sites for furin and the conserved Trp^{21}–Val^{22} cleavage site for ECE (Fig. 2A). The two active (21 aa) killifish EDN1s are 80% identical to human EDN1 and are 100% identical to each other (Fig. 2B). As seen in Fig. 1, our killifish preproEDN1s group with the other fish preproEDN1 sequences and group outside of the fish preproEDN2 and preproEDN3 sequences. We were unable to find a preproEDN orthologue in the *Ciona intestinalis* or *Branchiostoma* genomes, suggesting that the EDNs are found only in vertebrates.

We have sequenced 1696 bp from the middle of the killifish *ECE1* cDNA (accession no. EU009476). This translates into 565 aa from the killifish ECE1. Endothelin converting enzymes are found in all organism including Bacteria and Archaea (Fig. 3). As seen in Fig. 3, the non-vertebrate ECEs are not well resolved (i.e. lancelet ECE groups with locust and sea urchin, while sea squirt groups with hydra), and although there is no clear explanation for this, Fig. 3 shows three distinct ECE clades: ECE1, ECE2 and non-vertebrate ECE. Our partial

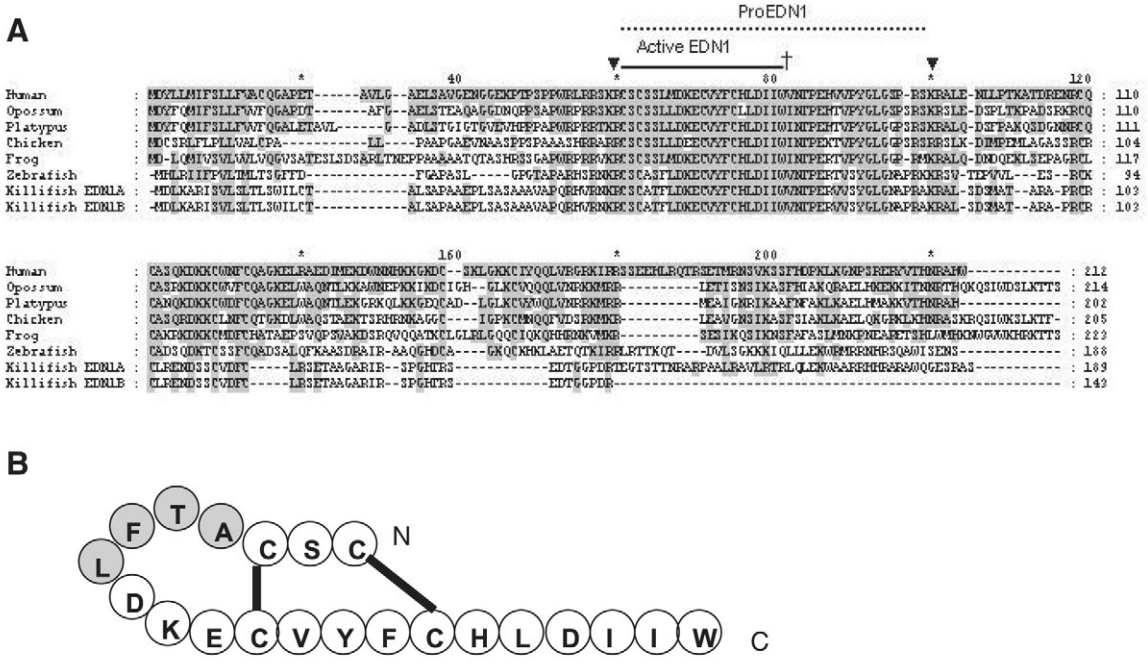

Fig. 2. An alignment of vertebrate preproendothelin-1 protein sequences. (A) Similar amino acid residues [based on the BLOSUM 62 score table (Eddy, 2004)] are highlighted in gray, as compared to human preproendothelin-1. The cleavage sites for furin (inverted triangles) and ECE1 (†) are indicated. Asterisks mark every 20th amino acid. (B) Predicted active EDN1 structure from the killifish, modeled after Webb (Webb, 1997). Amino acids different from human EDN1 are highlighted in gray. Two disulfide bonds are indicated at Cys^1–Cys^{15} and Cys^3–Cys^{10}. GenBank and Ensembl accession numbers are listed in Fig. 1, except for platypus EDN1, ENSOANP00000011454 and opossum EDN1, XP_001377153.1.

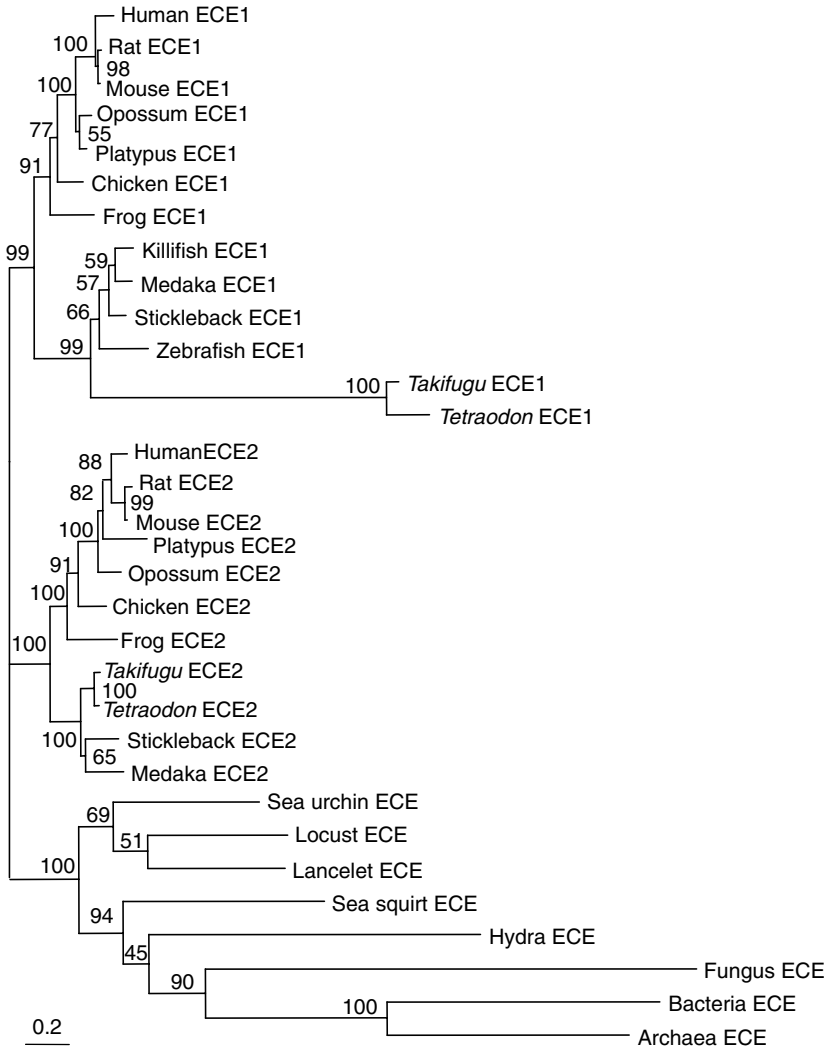

Fig. 3. Maximum likelihood analyses of the ECE family of proteins following the WAG model of amino acid substitutions (Whelan and Goldman, 2001), and a gamma distribution of 1.03. There are three distinct groups of ECE: ECE1, ECE2 and non-vertebrate ECE. Accession numbers: Archaea ECE, NP_616924; Bacteria ECE, NP_812722; chicken ECE1, NP_990048; chicken ECE2, ENSGALP00000010123; frog ECE1, AAH46653; frog ECE2, ENSXETP00000037627; fungus ECE, XP_754379; human ECE1, NP_001388; human ECE2, NP_055508; hydra ECE, AAD46624; killifish ECE1, EU009476; lancelet ECE, 86342 scaffold_150000101; locust ECE, AAN73018; medaka ECE2, ENSORLP00000025753; medaka ECE1, ENSORLP00000021332; mouse ECE1, NP_955011; mouse ECE2, NP_647454; opossum ECE1, ENSMODP00000019967; opossum ECE2, ENSMODP00000002887; platypus ECE1, ENSOANP00000023244; platypus ECE2, ENSOANP00000003016; rat ECE1, NP_446048; rat ECE2, NP_001002815; sea squirt ECE, ENSCSAVP00000016300; sea urchin ECE, XP_798822; stickleback ECE1, ENSGACP00000006069; stickleback ECE2, ENSGACP00000005922; *Takifugu* ECE1, NEWSINFRUP00000136873; *Takifugu* ECE2, NEWSINFRUP00000151424; *Tetraodon* ECE1, GSTENP00006535001; *Tetraodon* ECE2, CAG02177; zebrafish ECE1, XP_694687. Scale bar represents the number of replacements per site.

sequence of ECE1 from the killifish groups with the other fish ECE1 sequences confirming it is ECE1.

Tissue distributions

Using duplexing relative semi-quantitative PCR we found *EDN1A* mRNA in the gill, opercular epithelium, brain, heart, stomach, intestine and kidney of the killifish (Fig. 4). Relatively high expression was found in the gill, brain and kidney. *EDN1B* mRNA was not found in the opercular epithelium, and had very little expression in the gill, but was highly expressed in the brain, kidney and intestine. Finally, *ECE1* mRNA was found in all of the tissues tested, with highest expression in the stomach, intestine and gill (Fig. 4).

In situ hybridization

EDN1A mRNA was localized to gill epithelial cells in the interlamellar region (Fig. 5A). These cells were large, round and were dispersed along the entire length of the filament (not shown). *NKA* mRNA was also found in epithelial cells in the interlamellar region (Fig. 5C) but was concentrated only near the afferent filamental artery (trailing edge of the filament, not shown). The morphology of these *NKA* positive cells is consistent with mitochondrion-rich cells (MRCs) of the killifish gill (Katoh et al., 2001; Marshall, 2003; Choe et al., 2006; Hyndman et al., 2006). In contrast, *EDN1B* mRNA expression was rare (as was seen in the *EDN1B* tissue distribution described above); however, it was found in some lamellar pillar cells (Fig. 5D,F) and in epithelial cells adjacent to the environment (Fig. 5D). Incubation of slides with sense probes produced a little non-specific staining (Fig. 5B,E).

Immunohistochemistry

Proendothelin-1, the precursor to active EDN1, was immunolocalized to epithelial cells in the interlamellar region of the killifish gill, and on the lamellar pillar cells (Fig. 6A,C). Proendothelin-1 immunoreactivity was seen in epithelial cells adjacent to cells immunoreactive for NKA (Fig. 6A,C), and these cells share similar morphology to neuroendocrine cells (NECs) described in fishes (Zaccone et al., 1992; Goniakowska-Witalinska et al., 1995; Zaccone et al., 1996; Mauceri et al., 1999). This immunolocalization matches the killifish *EDN1* mRNA localization shown in Fig. 5. Slides incubated in NGS and double labeled with NKA were done as negative controls, and showed no non-specific staining of the proEDN1 secondary antibody and chromagen (Fig. 6B,D).

Salinity acclimations

When killifish were transferred from FW to SW there were no statistically significant changes in *EDN1A* or *EDN1B* mRNA levels over 24 h (acute acclimation) compared to sham (FW→FW) transfers (Fig. 7A,C). *ECE1* mRNA increased four- and sixfold compared with sham *ECE1* mRNA levels at 8 and 24 h post a FW→SW transfer (Fig. 7E). *EDN1A* mRNA levels did not change significantly with acute acclimation from SW→FW

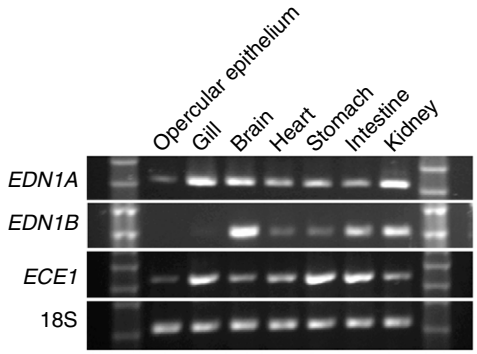

Fig. 4. Tissue distribution of killifish *EDN1A*, *EDN1B* and *ECE1* determined by duplexing semi-quantitative PCR with 18S as an internal control.

compared to sham (SW→SW) treatments (Fig. 7B), but 24 h *EDN1B* mRNA levels were almost threefold higher compared to sham *EDN1B* mRNA levels at 24 h (Fig. 7D). *ECE1* mRNA levels were twofold higher after 3 and 24 h of acclimation to FW but did not differ from sham values at 8 h post transfer (Fig. 7F). With chronic acclimation (30 days), there were no statistical differences between the SW- and FW-acclimated killifish for *EDN1A*, *EDN1B* or *ECE1* mRNA levels (Fig. 8). In addition, preproEDN1 (protein) immunolocalization did not differ between fish chronically acclimated to FW (Fig. 6A,B) or SW (Fig. 6C,D).

Discussion

Endothelin sequences

We have sequenced two cDNAs for *EDN1* from the killifish gill. These two transcripts have identical 5′ ends until base pair 510, where there is an AC insertion resulting in a frame shift mutation in *EDN1A* that changes the stop codon TGA to ACT GAG. Conversely, *EDN1B* may have lost an AC at position 510 resulting in a stop codon and a truncated preproEDN. Past this insertion/deletion (indel), the two transcripts differ along the rest of the sequence, but are only 5 bp different in total length. This suggests that the two transcripts are from duplicated *EDN1* genes and are not transcript variants. We did not find duplicate EDN1 genes in the *Takifugu*, *Tetraodon* or *Danio* genomes, suggesting the *EDN1* duplication was a *Fundulus*-specific event (see note added in proof). As a consequence of the indel at position 510, the predicted preproEDN-1a is 46 aa longer than preproEDN-1b. Even though there are differences between the killifish preproEDN-1s, the proEDN-1s and EDN1s are 100% identical. Why would a tissue (cell) produce two different mRNAs if the end protein translated is 100% identical? We hypothesize that these two EDN1s have remained in the killifish because they have different regulatory pathways, and/or are stimulated by different signals. This hypothesis might suggest that the *EDN1s* would have different tissue/cellular distributions. Supporting this hypothesis, from our tissue distribution analysis (Fig. 4), we found *EDN1a* was ubiquitously expressed in all the tissues tested, with relatively high expression in the gill, brain and kidney. Conversely, *EDN1b* was found in very low levels in the gill and opercular epithelium, but relatively high in the brain. Nevertheless, until complete killifish *EDN1A* and *EDN1B* genomic sequences are determined, it is unclear how and what factors may regulate these genes, and thus to suggest why these two have been retained in the killifish.

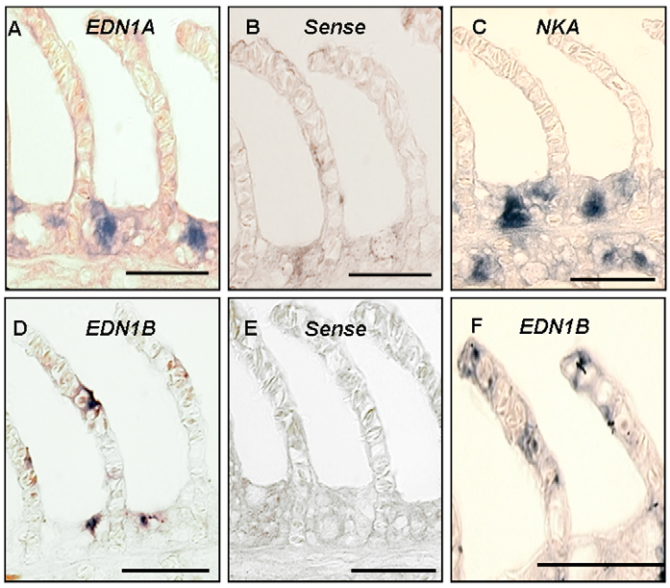

Fig. 5. Representative pictures of *in situ* hybridization of *EDN1A* and *EDN1B* mRNA in lamellar cross-sections of the seawater killifish gill. (A) The *EDN1A* antisense probe was localized to epithelial cells in the interlamellar region of the gill. Little staining was seen in the gill when the *EDN1A* sense probe was used (B). (C) The *NKA* antisense probe was localized to mitochondrion-rich cells. (D) *EDN1B* antisense probes bound to pillar cells and epithelial cells adjacent to the environment. Little staining was seen with the sense probe (E). (F) A magnification of the pillar cell *EDN1B* staining. Scale bars, 50 μm.

Gill expression of EDN1 mRNA and proEDN1 protein

In the killifish gill we found *EDN1A* mRNA expression in epithelial cells of the interlamellar region, and *EDN1B* mRNA expression was found in pillar cells, and in cells adjacent to the environment, in the interlamellar region. Not only are these two transcripts expressed in different levels within a tissue (Fig. 4), they are also expressed in different cells within the gill. From our immunohistochemical experiments, we found proEDN1 immunoreactivity in epithelial cells adjacent to the NKA immunoreactive cells. NKA is commonly used as a marker for the ion transporting, MRCs of the fish gill (Katoh et al., 2001; Marshall, 2003; Evans et al., 2005). Proendothelin immunoreactivity was also found on pillar cells, which is in agreement with our *in situ* hybridization findings. ProEDN was immunolocalized to gill neuroendocrine cells (NECs) of the eel (*Conger congo*), catfish (*Heteropneustes fossilis*) and dogfish (*Scyliorhfnus canicula*), and the morphology of these cells matches that of the proEDN immunoreactive epithelial cells in the killifish gill (Zaccone et al., 1996).

Endothelin production in the pillar cells was suspected by earlier workers (Sundin and Nilsson, 1998; Stenslokken et al., 1999), who showed that infusion of mammalian EDN1 into the lamellae of the rainbow trout resulted in a '*constriction of the vascular sheet*' (of the lamellae) and that this was likely due to

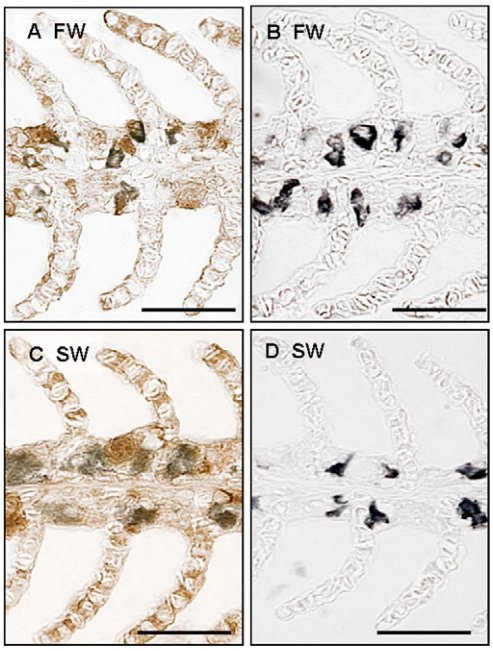

Fig. 6. Representative pictures of killifish lamellar cross-sections, labeled with anti-proendothelin-1 (brown) and anti-NKA (blue). (A,B) Gill sections from a chronic (>30 day) FW acclimated killifish and (C,D) a chronic SW acclimated killifish. (B,D) Sections were incubated in normal goat serum as a negative control for proendothelin immunoreactivity, and doubled labeled with anti-NKA (blue) to illustrate the position of the mitochondrion-rich cells (MRC) in the gill. Proendothelin immunoreactivity was found in a cell adjacent to the NKA immunoreactivity (MRC) and on gill pillar cells in both the FW and SW killifish. The immunoreactivity presented here matches the *in situ* hybridization of mRNA probes for *EDN1*s and *NKA* in Fig. 5. Scale bars, 50 μm.

constriction of the pillar cells. The authors hypothesized that hormonal control of pillar cell tone may be one mechanism to match respiratory needs of a fish while minimizing ion fluxes. There is no evidence that pillar cells are innervated (Bettex-Galland and Hughes, 1972; Bettex-Galland and Hughes, 1973); thus endocrine/paracrine/autocrine signaling molecules may be the regulators of pillar cell tone. Pillar cells contain contracting filamentous material (Bettex-Galland and Hughes, 1972; Bettex-Galland and Hughes, 1973) and recently an actin-binding protein was described, FHL5, that is highly expressed in these cells, suggesting that they are capable of contraction (Mistry et al., 2004). Video microscopy was used to demonstrate *in vivo* that pillar cells do contract with EDN1 infusion (Stenslokken et al., 1999). Recently, EDN receptors EDNRA and EDNRB were immunolocalized in the fish gill, and EDNRB was found throughout the gill vasculature, NECs and pillar cells of the cod *Gadus morhua* (Stenslokken et al., 2006). EDNRA was described in nerve fibers running along the length of the filament and innervating the gill vasculature (Stenslokken et al., 2006). In the fugu *Takifugu rubripes* EDNRA was found on the pillar cells and in erythrocytes (Sultana et al., 2007). Studies from our lab in the killifish have found EDNRB receptors throughout the gill vasculature and pillar cells, and EDNRA receptors on the mitochondrion-rich cell (K.A.H. and D.H.E., unpublished observations). In the long horn sculpin *Myoxocephalus octodecimspinosus*, EDNRA receptors were found on the pillar cells, while EDNRB was found throughout the gill vasculature (K.A.H. and D.H.E., unpublished observations). Evidently, there is species-specific EDN receptor distribution in the gill of fishes.

Acute and chronic salinity acclimations

Killifish usually live in estuaries where there are rapid changes in environmental conditions such as salinity and temperature (Marshall, 2003). We tested the effects of rapid changes of environmental salinity on mRNA expression of *EDN1A*, *EDN1B* and *ECE1*. *EDN1* transcript levels did not change with chronic acclimation to FW or SW (Fig. 8). In addition, proEDN1 immunoreactivity in the gill did not differ between SW and FW acclimated killifish (Fig. 6). However, *EDN1B* and *ECE1* mRNA levels increase with acute FW acclimation, suggesting that more active EDN1 protein is produced. 10^{-8} mol l^{-1} mammalian EDN1 can inhibit net chloride transport in the killifish opercular epithelium, and this is predominately due to stimulation of cyclo-oxygenase (COX) and subsequent prostaglandin production (Evans et al., 2004). These findings suggest that during transfer to a hypo-osmotic environment, EDN1B and ECE1 protein levels increase, resulting in an increase in active EDN1 that could potentially inhibit net chloride transport, helping the fish retain ions. However, we cannot rule out that EDN1 signaling in the gill is different than what was described in the killifish operculum (Evans et al., 2004) (see below). In addition, it is undetermined how volume stress, such as occurs during a rapid change to a hypo-osmotic environment, effects blood flow through the gill. *EDN1B* was found on gill pillar cells, and may play a role in regulating blood flow during blood volume increases; however, this is an unexplored area of fish gill physiology.

Although we found an increase in EDN1 during acclimation to FW, we unexpectedly found a sixfold increase in *ECE1* mRNA levels with acute SW acclimation, suggesting that there is an increase in ECE1 production during this period. This in turn would result in more EDN1 production because the proteolytic cleavage of proEDN1 to EDN1 by ECE1 is a rate-limiting step (D'Orleans-Juste et al., 2003). Our attempts to measure EDN1 production in the fish gill by enzyme immunoassay and Tris-Tricine western blotting were unsuccessful, but measurements of EDN1 levels are necessary to fully understand the role of EDN1 cell signaling in the fish gill. Recently, a 3.4-fold increase was shown in COX-2 mRNA levels in the killifish gill (Choe et al., 2006), 3 h post a FW→SW and a 2.6-fold increase 3 h post a SW→FW transfer, and the authors hypothesized that the increase in COX-2 is an important mechanism for gill cell survival during osmotic stress. A similar result has been demonstrated in mammalian medullary interstitial cells (that experience large changes in osmotic stress), which require functional COX-2 to survive (Hao et al., 1999; Hao et al., 2000). Medullary interstitial cells also contain EDNRs but do not produce EDN1 (Dean et al., 1996). Endothelin has been shown to stimulate COX-2 in a variety of mammalian tissues (Hughes et al., 1995; Chen et al., 2003), and EDN1 signaling *via* endothelial ENDRB results in the production of prostacyclin (Warner et al., 1989; Hirata et

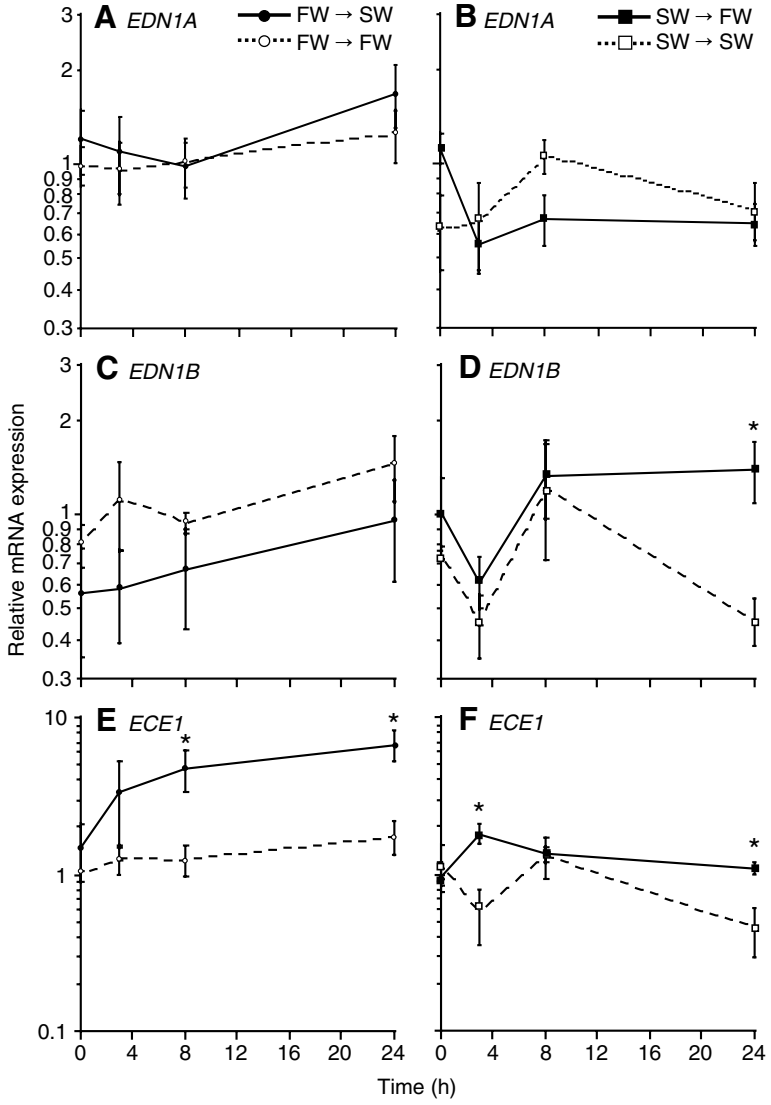

Fig. 7. Acute changes in killifish gill *EDN1A*, *EDN1B* and *ECE1* mRNA levels as determined by quantitative RT-PCR. FW→SW transfers are indicated by solid lines and solid circles and FW→FW sham controls are represented by open circles and dotted lines (A,C,E). SW→FW transfers are represented by solid lines and solid squares and SW→SW sham controls by dotted lines and open squares (B,D,F). *N*=5 or 6 killifish per time and treatment and values are means ± s.e.m. Note the *y* axis is logarithmic. All values are normalized to L8 and standardized to chronic SW mRNA levels (see Fig. 9). (A,B) *EDN1A* mRNA levels, (C,D) *EDN1B* mRNA levels and (E,F) *ECE1* mRNA levels. The asterisks indicate statistical significance ($P<0.05$) compared to sham value.

al., 1993). Taken together, our findings suggest that during rapid changes in environmental salinity, gill cell survival during this osmotic stress may be accomplished by increased EDN1 production and subsequent stimulation of COX production of prostaglandins. To the best of our knowledge, it is unclear what aids cell survival during salt or water load in fishes, and it is plausible, since EDN1 and ECE1 are ubiquitously expressed, that this may be a more global change in their signaling patterns and is not a gill-specific phenomenon; however, this is yet to be determined and experiments testing these hypotheses are needed. In addition, studies blocking aspects of EDN1 signaling in the gill and subjecting these fish to salinity challenges are vital in understanding EDN1 function during osmotic stress. This technique has been successful in mice models, where kidney collecting duct EDN1 (or EDNRB1) knockout mice who are fed a high salt diet are unable to excrete the excess Na^+ accumulated and are severely hypertensive (Ahn et al., 2004; Ge et al., 2006), suggesting that EDN1 is necessary for salt excretion in mammals. Applications of these types of techniques to fish models are necessary to fully understand the *in vivo* role of EDN signaling in the fish gill.

Evolution of EDNs and ECE

While searching the completed genome projects, we were unable to find EDN orthologues in any organism basal to the teleost fishes. From the maximum likelihood analyses presented in Fig. 1, there are three distinct groups, representing preproEDN1, preproEDN2 and preproEDN3 in vertebrates. Aortic vascular smooth muscle rings from the sea lamprey and Atlantic hagfish constrict in response to mammalian EDN1, suggesting that the receptors and EDN1 are expressed endogenously in these basal, Agnathan vertebrates (Evans and Harrie, 2001). Physiological responses to EDN1 have also been demonstrated in the spiny dogfish shark (Evans et al., 1996; Evans and Gunderson, 1999), again suggesting that EDN1 is produced endogenously. Currently, the exact evolutionary history of this family of peptides is not clear. EDN sequences from hagfish, lamprey and sharks are necessary to determine when these peptides arose, and to determine if it was due to gene/genome duplications or other evolutionary events over vertebrate evolution. Interestingly, mutations in EDN1, endothelin receptors (EDNRs) or ECE result in severe craniofacial developmental abnormalities, and these phenotypes are often lethal (Kurihara et al., 1994; Brand et al., 1998; Clouthier and Schilling, 2004; Nair et al., 2007), suggesting the EDN signaling is necessary for development in vertebrates, and it may be a key innovation in the radiation of vertebrates.

Unlike EDNs, which are only found in vertebrates, ECE is found in all organisms, including Bacteria and Archaea. In Fig. 3, our maximum likelihood analyses reveal three distinct groups of ECEs: prokaryote, fungal and invertebrate ECE, vertebrate ECE1 and vertebrate ECE2. This suggests a gene duplication event sometime after the chordate–vertebrate split, but before the teleost radiation. Since there is no molecular evidence for EDNs or EDNRs in animals basal to the vertebrates why would they have an ECE? Endothelin converting enzymes are zinc-dependant metalloendoproteases and part of the Neprelysin and Kell family (Shimada et al., 1994; Xu et al., 1994). In vertebrates, ECE can function as a monomer or dimer; however, for effective proteolytic cleavage of proEDN1 to EDN1,

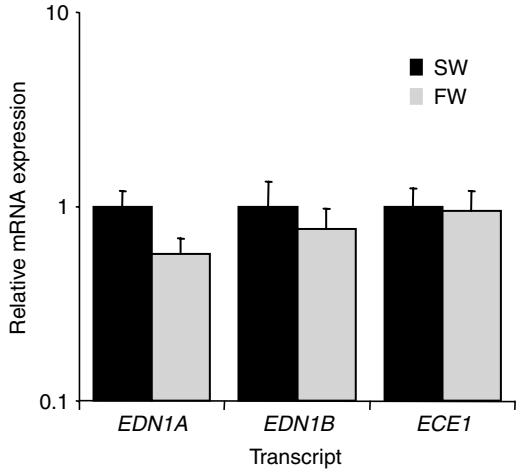

Fig. 8. Chronic changes in gill *EDN1A*, *EDN1B* and *ECE1* mRNA levels as measured by quantitative RT-PCR. Killifish (N=6) were transferred from FW→SW (SW treatment, black bars) or SW→FW (FW treatment, gray bars) and sacrificed 30 days later. Values are means ± s.e.m. Note the y axis is logarithmic. No significant changes in mRNA level were found between the SW and FW killifish for *EDN1A*, *EDN1B* or *ECE1*.

dimerization at Cys^{412} is preferential (Shimada et al., 1996). In contrast, hydra ECE (Zhang et al., 2001) and the other invertebrate, fungal and prokaryote ECEs are missing Cys^{412} and are believed to function as monomers (Zhang et al., 2001). Vertebrate ECE has been shown to cleave peptides other than proEDN, including bradykinin, angiotensin I and substance P (Hoang and Turner, 1997; Johnson et al., 1999), suggesting that ECE may be a generalist protease. Although the native substrates cleaved by ECE in non-vertebrate organisms are undetermined, it is plausible that ECE originally cleaved substrates found in all organisms, and during vertebrate evolution started functioning as a dimer and preferentially cleaving proEDN.

Tentative model for EDN1 signaling in the killifish gill

To summarize our findings, we propose the following model (Fig. 9) of paracrine and autocrine EDN1 signaling in the fish gill. The diagram shows a lamellar cross-section of the gill (same orientation as the gills in Figs 5–7), with pillar cells (PCs) highlighted in grey and adjacent pavement cells (PVCs) in white. In the intralemallar region there are two MRCs and an NEC above the gill vasculature. Cyclo-oxygenase-2 (COX-2) and neuronal nitric oxide synthase (nNOS) were previously immunolocalized in the killifish gill, to MRCs (Choe et al., 2006) and NECs, nerve fibers and lamellar arterioles (LA) (Hyndman et al., 2006), respectively. NKA was immunolocalized to the basolateral membrane of the MRC (see Katoh et al., 2001; Choe et al., 2006; Hyndman et al., 2006) and the chloride channel, cystic fibrosis transmembrane conductance regulator (CFTR), to the apical membrane of the MRC (Katoh et al., 2001). From our studies and others, EDNRB were found throughout the gill vasculature (K.A.H. and D.H.E., unpublished) (Stenslokken et al., 2006), and EDNRB and EDNRA were on the pillar cells, depending on the species (K.A.H. and D.H.E., unpublished observations) (Stenslokken et al., 2006; Sultana et al., 2007). EDNRA were found on MRCs in the killifish gill (K.A.H. and D.H.E., unpublished observations). Here we present EDN1 expression in cells adjacent to the MRC (likely NECs) and pillar cells. This suggests a paracrine role of EDN1 signaling, given that it is produced in the NEC and can bind to receptors on the adjacent MRCs (Fig. 9, pathway 1) where it potentially stimulates COX-2 activity, resulting in cell survival during osmotic stress and/or alter ion transport by the MRC as previously hypothesized (Evans et al., 2004). EDN1 can also potentially act as a paracrine binding to EDNRB receptors on the gill vasculature and lamellar arterioles, suggesting it can regulate perfusion of the lamellae (Fig. 9, pathway 1). It also can act as an autocrine on the pillar

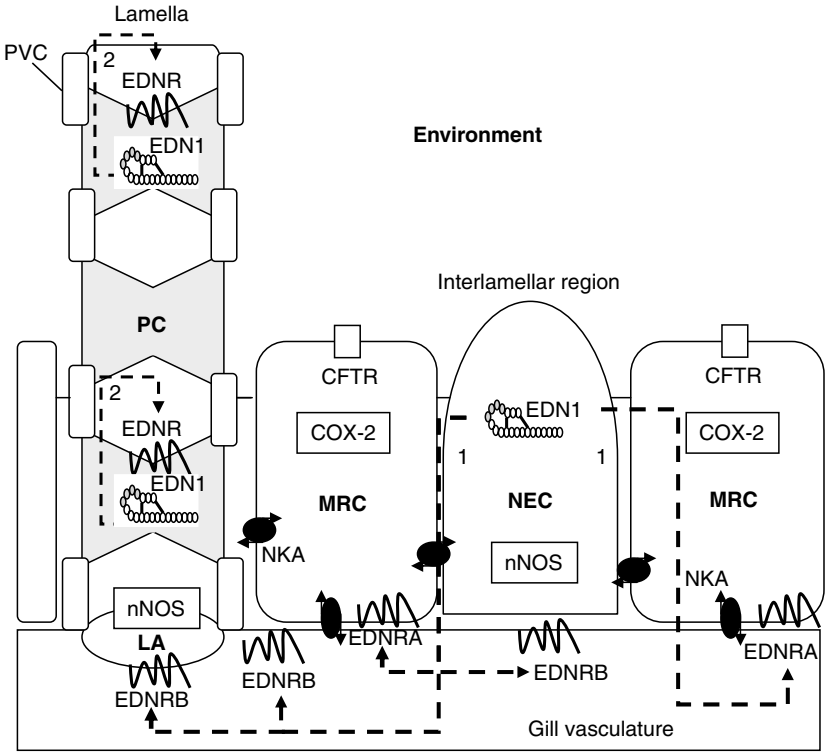

Fig. 9. A model of paracrine and autocrine EDN1 signaling in the fish gill. The diagram shows a lamellar cross-section (see Figs 5–7) with pillar cells (PCs) in gray, pavement cells (PVCs) and a lamellar arteriole (LA) adjacent to the interlamellar region of the gill containing mitochondrion rich-cells (MRCs), a neuroendocrine cell (NEC), and the gill vasculature. Cyclo-oxygenase-2 (COX-2) and neuronal nitric oxide were previously immunolocalized in the killifish gill (Choe et al., 2006; Hyndman et al., 2006). NKA and the cystic fibrosis transmembrane conductance regulator (CFTR) are used as markers for the MRC (Katoh et al., 2001). See text for details.

cells, further supporting the role of regulation of local perfusion across a lamella to meet the respiratory needs of the fish (Fig. 9, pathway 2) (Sundin and Nilsson, 1998; Stenslokken et al., 1999). It may also help maintain lamella integrity during rapid increases in plasma volume during exposure to a hypo-osmotic environment. This is the first model to depict EDN1 signaling in the fish gill, and in the future, studies determining the specific function of EDN1 in the gill and whole fish, are necessary to understand its role in normal fish physiology.

List of abbreviations and symbols

CFTR	cystic fibrosis transmembrane conductance regulator
COX	cyclo-oxygenase
CT	cycle threshold
DIG	digoxigenin
E	efficiency
ECE	endothelin converting enzyme
EDN	endothelin
EDNRA	endothelin receptor A
EDNRB1	endothelin receptor B1
EDNRB2	endothelin receptor B2
EDNRC	endothelin C receptor
indel	insertion/deletion
LA	lamellar arteriole
MRC	mitochondrion-rich cell
NEC	neuroendocrine cell
NKA	sodium, potassium ATPase
nNOS	neuronal nitric oxide synthase
ORF	open reading frame
PC	pillar cell
preproEDN	preproendothelin
proEDN	proendothelin
PVC	pavement cell
qRT-PCR	quantitative real-time polymerase chain reaction
UTR	untranslated region

We thank Dr Michael Miyamoto for guidance with our phylogenetic analyses, and Dr Keith Choe for his help with molecular biology. We also thank Drs Michael McCoy and Michelle Monette for their statistical analysis advice. Funding was provided by NSF IOB-0519579 to D.H.E. and Simga Xi GIAR to K.A.H.

Note added in proof

Since this paper was submitted, we have found *EDN1* duplicate genes in the zebrafish, stickleback, *Takifugu* and Medaka genome projects (Ensembl e!47), suggesting that this is not necessarily a killifish-specific duplicate as we initially thought. This may be the result of a teleost-specific genome duplication event that occurred after the split from the ancestor leading to the tetrapods.

Ensembl numbers:

zebrafish	ENSDARP00000093511
stickleback	ENSGACP00000017902
Takifugu	SINFRUP00000152472
Medaka	ENSORLP00000011633.

References

Ahn, D., Ge, Y., Stricklett, P. K., Gill, P., Taylor, D., Hughes, A. K., Yanagisawa, M., Miller, L., Nelson, R. D. and Kohan, D. E. (2004). Collecting duct-specific knockout of endothelin-1 causes hypertension and sodium retention. *J. Clin. Invest.* **114**, 504-511.

Arai, H., Hori, S., Aramori, I., Ohkubo, H. and Nakanishi, S. (1990). Cloning and expression of a cDNA encoding an endothelin receptor. *Nature* **348**, 730-732.

Bettex-Galland, M. and Hughes, G. M. (1972). Demonstration of a contractile actomyosin-like protein in pillar cells of fish gills. *Experientia* **28**, 744.

Bettex-Galland, M. and Hughes, G. M. (1973). Contractile filamentous material in the pillar cells of fish gills. *J. Cell Sci.* **13**, 359-370.

Brand, M., Le Moullec, J. M., Corvol, P. and Gasc, J. M. (1998). Ontogeny of endothelins-1 and -3, their receptors, and endothelin converting enzyme-1 in the early human embryo. *J. Clin. Invest.* **101**, 549-559.

Chen, D. H., Balyakina, E. V., Lawrence, M., Christman, B. W. and Meyrick, B. (2003). Cyclooxygenase is regulated by ET-1 and MAPKs in peripheral lung microvascular smooth muscle cells. *Am. J. Physiol.* **284**, L614-L621.

Chenna, R., Sugawara, H., Koike, T., Lopez, R., Gibson, T. J., Higgins, D. G. and Thompson, J. D. (2003). Multiple sequence alignment with the Clustal series of programs. *Nucleic Acids Res.* **31**, 3497-3500.

Choe, K. P. and Evans, D. H. (2003). Compensation for hypercapnia by a euryhaline elasmobranch: effect of salinity and roles of gills and kidneys in fresh water. *J. Exp. Zool. A* **297**, 52-63.

Choe, K. P., Verlander, J. W., Wingo, C. S. and Evans, D. H. (2004). A putative H^+-K^+-ATPase in the Atlantic stingray, *Dasyatis sabina*: primary sequence and expression in gills. *Am. J. Physiol.* **287**, R981-R991.

Choe, K. P., Kato, A., Hirose, S., Plata, C., Sindic, A., Romero, M. F., Claiborne, J. B. and Evans, D. H. (2005). NHE3 in an ancestral vertebrate: primary sequence, distribution, localization, and function in gills. *Am. J. Physiol.* **289**, R1520-R1534.

Choe, K. P., Havird, J., Rose, R., Hyndman, K., Piermarini, P. and Evans, D. H. (2006). COX2 in a euryhaline teleost, *Fundulus heteroclitus*: primary sequence, distribution, localization, and potential function in gills during salinity acclimation. *J. Exp. Biol.* **209**, 1696-1708.

Clouthier, D. E. and Schilling, T. F. (2004). Understanding endothelin-1 function during craniofacial development in the mouse and zebrafish. *Birth Defects Res. C Embryo Today* **72**, 190-199.

D'Orleans-Juste, P., Plante, M., Honore, J. C., Carrier, E. and Labonte, J. (2003). Synthesis and degradation of endothelin-1. *Can. J. Physiol. Pharmacol.* **81**, 503-510.

Dean, R., Zhuo, J., Alcorn, D., Casley, D. and Mendelsohn, F. A. (1996). Cellular localization of endothelin receptor subtypes in the rat kidney following *in vitro* labelling. *Clin. Exp. Pharmacol. Physiol.* **23**, 524-531.

Eddy, S. R. (2004). Where did the BLOSUM62 alignment score matrix come from? *Nat. Biotechnol.* **22**, 1035-1036.

Evans, D. H. (2001). Vasoactive receptors in abdominal blood vessels of the dogfish shark, *Squalus acanthias*. *Physiol. Biochem. Zool.* **74**, 120-126.

Evans, D. H. and Gunderson, M. P. (1999). Characterization of an endothelin ET(B) receptor in the gill of the dogfish shark *Squalus acanthias*. *J. Exp. Biol.* **202**, 3605-3610.

Evans, D. H. and Harrie, A. C. (2001). Vasoactivity of the ventral aorta of the American eel (*Anguilla rostrata*), Atlantic hagfish (*Myxine glutinosa*), and sea lamprey (*Petromyzon marinus*). *J. Exp. Zool.* **289**, 273-284.

Evans, D. H., Gunderson, M. and Cegelis, C. (1996). ETB-type receptors mediate endothelin-stimulated contraction in the aortic vascular smooth muscle of the spiny dogfish shark, *Squalus acanthias*. *J. Comp. Physiol. B* **165**, 659-664.

Evans, D. H., Rose, R. E., Roeser, J. M. and Stidham, J. D. (2004). NaCl transport across the opercular epithelium of *Fundulus heteroclitus* is inhibited by an endothelin to NO, superoxide, and prostanoid signaling axis. *Am. J. Physiol.* **286**, R560-R568.

Evans, D. H., Piermarini, P. M. and Choe, K. P. (2005). The multifunctional fish gill: dominant site of gas exchange, osmoregulation, acid-base regulation, and excretion of nitrogenous waste. *Physiol. Rev.* **85**, 97-177.

Ge, Y., Bagnall, A., Stricklett, P. K., Strait, K., Webb, D. J., Kotelevtsev, Y. and Kohan, D. E. (2006). Collecting duct-specific knockout of the endothelin B receptor causes hypertension and sodium retention. *Am. J. Physiol.* **291**, F1274-F1280.

Goniakowska-Witalinska, L., Zaccone, G., Fasulo, S., Mauceri, A., Licata, A. and Youson, J. (1995). Neuroendocrine cells in the gills of the bowfin *Amia calva*. An ultrastructural and immunocytochemical study. *Folia Histochem. Cytobiol.* **33**, 171-177.

Guindon, S., Lethiec, F., Duroux, P. and Gascuel, O. (2005). PHYML Online – a web server for fast maximum likelihood-based phylogenetic inference. *Nucleic Acids Res.* **33**, W557-W559.

Hao, C. M., Komhoff, M., Guan, Y., Redha, R. and Breyer, M. D. (1999). Selective targeting of cyclooxygenase-2 reveals its role in renal medullary interstitial cell survival. *Am. J. Physiol.* **277**, F352-F359.

Hao, C. M., Yull, F., Blackwell, T., Komhoff, M., Davis, L. S. and Breyer, M. D. (2000). Dehydration activates an NF-kappaB-driven, COX2-dependent survival mechanism in renal medullary interstitial cells. *J. Clin. Invest.* **106**, 973-982.

Hirata, Y., Emori, T., Eguchi, S., Kanno, K., Imai, T., Ohta, K. and Marumo, F. (1993). Endothelin receptor Subtype-B mediates synthesis of nitric-oxide by cultured bovine endothelial-cells. *J. Clin. Invest.* **91**, 1367-1373.

Hoang, M. V. and Turner, A. J. (1997). Novel activity of endothelin-converting enzyme: hydrolysis of bradykinin. *Biochem. J.* **327**, 23-26.

Hughes, A. K., Padilla, E., Kutchera, W. A., Michael, J. R. and Kohan, D. E. (1995). Endothelin-1 induction of cyclooxygenase-2 expression in rat mesangial cells. *Kidney Int.* **47**, 53-61.

Hyndman, K. A., Choe, K. P., Havird, J. C., Rose, R. E., Piermarini, P. M. and Evans, D. H. (2006). Neuronal nitric oxide synthase in the gill of the killifish, *Fundulus heteroclitus*. *Comp. Biochem. Physiol.* **144B**, 510-519.

Johnson, G. D., Stevenson, T. and Ahn, K. (1999). Hydrolysis of peptide hormones by endothelin-converting enzyme-1. A comparison with neprilysin. *J. Biol. Chem.* **274**, 4053-4058.

Karnaky, K. J., Jr, Degnan, K. J. and Zadunaisky, J. A. (1977). Chloride transport across isolated opercular epithelium of killifish: a membrane rich in chloride cells. *Science* **195**, 203-205.

Karne, S., Jayawickreme, C. K. and Lerner, M. R. (1993). Cloning and characterization of an endothelin-3 specific receptor (ETC receptor) from *Xenopus laevis* dermal melanophores. *J. Biol. Chem.* **268**, 19126-19133.

Katoh, F., Hasegawa, S., Kita, J., Takagi, Y. and Kaneko, T. (2001). Distinct seawater and freshwater types of chloride cells in killifish, *Fundulus heteroclitus*. *Can. J. Zool.* **79**, 822-829.

Kimura, S., Kasuya, Y., Sawamura, T., Shinimi, O., Sugita, Y., Yanagisawa, M., Goto, K. and Masaki, T. (1989). Conversion of big endothelin-1 to 21-residue endothelin-1 is essential for expression of full vasoconstrictor activity: structure-activity relationships of big endothelin-1. *J. Cardiovasc. Pharmacol.* **13** Suppl. 5, S5-S7, discussion S18.

Kurihara, Y., Kurihara, H., Suzuki, H., Kodama, T., Maemura, K., Nagai, R., Oda, H., Kuwaki, T., Cao, W. H., Kamada, N. et al. (1994). Elevated blood pressure and craniofacial abnormalities in mice deficient in endothelin-1. *Nature* **368**, 703-710.

Lecoin, L., Sakurai, T., Ngo, M. T., Abe, Y., Yanagisawa, M. and Le Douarin, N. M. (1998). Cloning and characterization of a novel endothelin receptor subtype in the avian class. *Proc. Natl. Acad. Sci. USA* **95**, 3024-3029.

Marshall, W. S. (2003). Rapid regulation of NaCl secretion by estuarine teleost fish: coping strategies for short-duration freshwater exposures. *Biochim. Biophys. Acta* **1618**, 95-105.

Masereeuw, R., Terlouw, S. A., van Aubel, R. A., Russel, F. G. and Miller, D. S. (2000). Endothelin B receptor-mediated regulation of ATP-driven drug secretion in renal proximal tubule. *Mol. Pharmacol.* **57**, 59-67.

Mauceri, A., Fasulo, S., Ainis, L., Licata, A., Lauriano, E. R., Martinez, A., Mayer, B. and Zaccone, G. (1999). Neuronal nitric oxide synthase (nNOS) expression in the epithelial neuroendocrine cell system and nerve fibers in the gill of the catfish, *Heteropneustes fossilis*. *Acta Histochem.* **101**, 437-448.

Miller, D. S., Masereeuw, R. and Karnaky, K. J., Jr (2002). Regulation of MRP2-mediated transport in shark rectal salt gland tubules. *Am. J. Physiol.* **282**, R774-R781.

Mistry, A. C., Kato, A., Tran, Y. H., Honda, S., Tsukada, T., Takei, Y. and Hirose, S. (2004). FHL5, a novel actin-binding protein, is highly expressed in eel gill pillar cells and responds to wall tension. *Am. J. Physiol.* **287**, R1141-R1154.

Nair, S., Li, W., Cornell, R. and Schilling, T. F. (2007). Requirements for Endothelin type-A receptors and Endothelin-1 signaling in the facial ectoderm for the patterning of skeletogenic neural crest cells in zebrafish. *Development* **134**, 335-345.

Olson, K. R., Duff, D. W., Farrell, A. P., Keen, J., Kellogg, M. D., Kullman, D. and Villa, J. (1991). Cardiovascular effects of endothelin in trout. *Am. J. Physiol.* **260**, H1214-H1223.

Opgenorth, T. J., Wu-Wong, J. R. and Shiosaki, K. (1992). Endothelin-converting enzymes. *FASEB J.* **6**, 2653-2659.

Pfaffl, M. W. (2001). A new mathematical model for relative quantification in real-time RT-PCR. *Nucleic Acids Res.* **29**, e45.

Piermarini, P. M., Verlander, J. W., Royaux, I. E. and Evans, D. H. (2002). Pendrin immunoreactivity in the gill epithelium of a euryhaline elasmobranch. *Am. J. Physiol.* **283**, R983-R992.

Rose, T. M., Henikoff, J. G. and Henikoff, S. (2003). CODEHOP (COnsensus-DEgenerate Hybrid Oligonucleotide Primer) PCR primer design. *Nucleic Acids Res.* **31**, 3763-3766.

Sakurai, T., Yanagisawa, M., Takuwa, Y., Miyazaki, H., Kimura, S., Goto, K. and Masaki, T. (1990). Cloning of a cDNA-encoding a non-isopeptide-selective subtype of the endothelin receptor. *Nature* **348**, 732-735.

Shimada, K., Takahashi, M. and Tanzawa, K. (1994). Cloning and functional expression of endothelin-converting enzyme from rat endothelial cells. *J. Biol. Chem.* **269**, 18275-18278.

Shimada, K., Takahashi, M., Turner, A. J. and Tanzawa, K. (1996). Rat endothelin-converting enzyme-1 forms a dimer through Cys412 with a similar catalytic mechanism and a distinct substrate binding mechanism compared with neutral endopeptidase-24.11. *Biochem. J.* **315**, 863-867.

Stenslokken, K. O., Sundin, L. and Nilsson, G. E. (1999). Cardiovascular and gill microcirculatory effects of endothelin-1 in atlantic cod: evidence for pillar cell contraction. *J. Exp. Biol.* **202**, 1151-1157.

Stenslokken, K. O., Sundin, L. and Nilsson, G. E. (2006). Endothelin receptors in teleost fishes: cardiovascular effects and branchial distribution. *Am. J. Physiol.* **290**, R852-R860.

Sultana, N., Nag, K., Kato, A. and Hirose, S. (2007). Pillar cell and erythrocyte localization of fugu ET(A) receptor and its implication. *Biochem. Biophys. Res. Commun.* **355**, 149-155.

Sundin, L. and Nilsson, G. E. (1998). Endothelin redistributes blood flow through the lamellae of rainbow trout gills. *J. Comp. Physiol. B* **168**, 619-623.

Wang, H., Quan, J., Kotake-Nara, E., Uchide, T., Andoh, T. and Saida, K. (2006). cDNA cloning and sequence analysis of preproendothelin-1 (PPET-1) from salmon, *Oncorhynchus keta*. *Exp. Biol. Med. Maywood* **231**, 709-712.

Wang, Y., Jensen, J., Abel, P. W., Fournier, A., Holmgren, S. and Conlon, J. M. (2001). Effects of trout endothelin on the motility of gastrointestinal smooth muscle from the trout and rat. *Gen. Comp. Endocrinol.* **123**, 156-162.

Warner, T. D., Mitchell, J. A., de Nucci, G. and Vane, J. R. (1989). Endothelin-1 and endothelin-3 release EDRF from isolated perfused arterial vessels of the rat and rabbit. *J. Cardiovasc. Pharmacol.* 13 Suppl. 5, S85-S88, discussion S102.

Webb, D. J. (1997). Endothelin: from molecule to man. *Br. J. Clin. Pharmacol.* **44**, 9-20.

Whelan, S. and Goldman, N. (2001). A general empirical model of protein evolution derived from multiple protein families using maximum-likelihood approach. *Mol. Biol. Evol.* **18**, 691-699.

Xu, D., Emoto, N., Giaid, A., Slaughter, C., Kaw, S., deWit, D. and Yanagisawa, M. (1994). ECE-1: a membrane-bound metalloprotease that catalyzes the proteolytic activation of big endothelin-1. *Cell* **78**, 473-485.

Yanagisawa, M., Kurihara, H., Kimura, S., Tomobe, Y., Kobayashi, M., Mitsui, Y., Yazaki, Y., Goto, K. and Masaki, T. (1988). A novel potent vasoconstrictor peptide produced by vascular endothelial cells. *Nature* **332**, 411-415.

Zaccone, G., Lauweryns, J. M., Fasulo, S., Tagliafierro, G., Ainis, L. and Licata, A. (1992). Immunocytochemical localization of serotonin and neuropeptides in the neuroendocrine paraneurons of teleost and lungfish gills. *Acta Zool.* **73**, 177-183.

Zaccone, G., Mauceri, A., Fasulo, S., Ainis, L., Lo Cascio, P. and Ricca, M. B. (1996). Localization of immunoreactive endothelin in the neuroendocrine cells of fish gill. *Neuropeptides* **30**, 53-57.

Zeidel, M. L., Brady, H. R., Kone, B. C., Gullans, S. R. and Brenner, B. M. (1989). Endothelin, a peptide inhibitor of Na(+)-K(+)-ATPase in intact renaltubular epithelial cells. *Am. J. Physiol.* **257**, C1101-C1107.

Zhang, J., Leontovich, A. and Sarras, M. P., Jr (2001). Molecular and functional evidence for early divergence of an endothelin-like system during metazoan evolution: analysis of the Cnidarian, hydra. *Development* **128**, 1607-1615.